https://www.scirp.org/journal/ns Natural Science, 2021, Vol. 13, (No. 9), pp: 437-449

Stress Field Changes before the M_S8.0 Wenchuan Earthquake

Anfu Niu, Jing Zhao, Yan Wei, Zhengyi Yuan, Ping Ji

China Earthquake Networks Center, Beijing, China

Correspondence to: Jing Zhao, zhaojing@seis.ac.cn; Yan Wei, ywpro@163.com

Keywords: Wenchuan Earthquake, Stress Field, Benioff Creep, Global Navigation Satellite System (GNSS)
Received: June 23, 2021 **Accepted:** September 25, 2021 **Published:** September 28, 2021

ABSTRACT

The apparent lack of pre-seismic crustal deformation preceding the 2008 M_S8.0 Wenchuan earthquake has been the subject of debate. In this study, tiltmeter data recorded close to the earthquake epicenter were analysed using spectrum and wavelet analysis. Changes in the stress field before the earthquake were analyzed based on the Benioff creep release and changes in regional Global Navigation Satellite System (GNSS) baselines. The characteristics of far- and near-field seismicity and deformation processes were investigated using rock fracture experiments. The results show that during pre-seismic strain energy accumulation, there was a synergy between stress field changes both proximal and distal to the epicenter; moreover, we identified a strong correlation between Benioff creep release and shortening of the LUZH-GUAN GNSS baseline. During the sub-instability stage, the deformation characteristics of different structural sectors differed; faults near the epicenter were in a highly locked state, and the deformation rate and wave spectra of main period waves obviously decreased. This reflects fixed point deformation driven by deep stress. These results are of great significance for understanding geophysical field observations, for clarifying pre-seismic deformation and for earthquake prediction.

1. INTRODUCTION

The M_S8.0 Wenchuan earthquake of 12 May 2008 occurred along the NE trending Longmenshan fault zone, located in the center of an N-S seismic belt of the eastern Qinghai-Tibet Plateau, on the southeastern boundary of the Bayan Har block. According to seismo-geological research, a 240 km surface fracture zone formed along the Longmenshan central fault and front fault owing to the earthquake [1]. The seismic fault movement was dominated by thrust and dextral strike slip components, with 4 - 6 m of coseismic vertical displacement and 3 - 5 m of dextral horizontal displacement [1, 2]. However, no reliable precursory signals or anomalous shallow activity were identified; that is, shallow processes did not match the deep processes

associated with the earthquake. Teng *et al.* [3] proposed a deep dynamic process model of the earthquake, and raised a number of questions; in particular, did geophysical field observations record abnormal changes before the earthquake?

According to the characteristics of coseismic and tectonic deformation, the theory of earthquake prediction by monitoring fault pre-slip was first proposed in the 1960s [4]. Many scholars believe that seismogenic faults always experience pre-slip before an earthquake. However, Johnston *et al.* [5] and Amoruso and Crescentini [6] found that even when installed in the epicenter area, high-precision strain gauges do not always detect the expected acceleration of strain expansion (on a scale of days) [7] or nucleation area expansion (on a scale of hundredths of a second to seconds) [8]. Before the 2008 Wenchuan earthquake, precursory deformation in the epicentral region was more limited than that in peripheral areas [9]; which gives rise to questions around identifying and monitoring precursory deformation before large earthquakes [10-12].

The crustal stress field consists of *in situ* stress and transient stress. *In situ* stress, also known as static stress or absolute stress, is caused by tectonic movement over a long (geological) timescale. Transient stress, also known as dynamic stress, is mainly derived from crustal stress processes caused by the Earth's deep medium rheology, and short-term interaction of the Earth's crust and mantle with seismic waves; transient stress fluctuates significantly. Slow earthquakes, which have periods of tens of seconds to hours or even days, and long-period deformation waves, which have periods of days to months, are reflections of the transient stress field [13-16]. In addition, variables such as the coseismic velocity field and gravity field, along with observations of ground tilt, strain, gravity, and Global Navigation Satellite System (GNSS) data can also reflect the transient stress field and its short-term characteristic in a given region [13-16]. For this reason, the characteristics of pre-seismic crustal deformation differ from those of coseismic or tectonic deformation. Improved understanding of deep earthquake dynamics has become a research focus [3].

Based on the analysis of pre-seismic deformation data from China, the USA, Japan, and the former Soviet Union, Wu *et al.* [17] summarized three pre-seismic deformation stages—α, β, and γ—corresponding to long-, medium-, and short-term precursors, respectively. Ma *et al.* [18, 19] and Ren *et al.* [20] provided evidence of fault sub-instability (corresponding to the γ stage) before large earthquakes based on rock fracturing experiments. Using actual observation data, a number of studies have investigated the deformation characteristics of the sub-instability stage [20-22]; however, research on deep deformation in epicentral regions and its impact on the regional stress field is rare.

2. OVERVIEW OF THE STUDY AREA

2.1. Epicenter Area of the Wenchuan Earthquake

The tectonic setting and dynamic background of the Wenchuan earthquake have been studied by many authors [3, 23]. The Wenchuan deformation observation station, located on the back fault of the Longmenshan fault belt, was the closest deformation observation station to the epicenter of the 2008 M_S8.0 Wenchuan earthquake (**Figure 1**). During the earthquake, the monitoring station was seriously damaged and it is no longer in use.

2.2. External Stress Field

Using the finite element numerical simulation method, Zhang *et al.* [24] analyzed strain field changes caused by the M_S8.1 Kunlun Mountain earthquake on 14 November 2001, and the effect on subsequent earthquakes. This event occurred on the western boundary of the Bayan Har block and the regional stress field was significantly affected, with seismicity in the epicentral region significantly enhanced. The 2008 Wenchuan earthquake, which occurred on the eastern boundary of the Bayan Har block, was likely triggered by the 2001 Kunlun Mountain earthquake.

Therefore, we chose the time-stamp of the M_S8.1 Kunlun Mountain earthquake as the starting point for our analysis, and the area of enhanced seismicity as our research area.

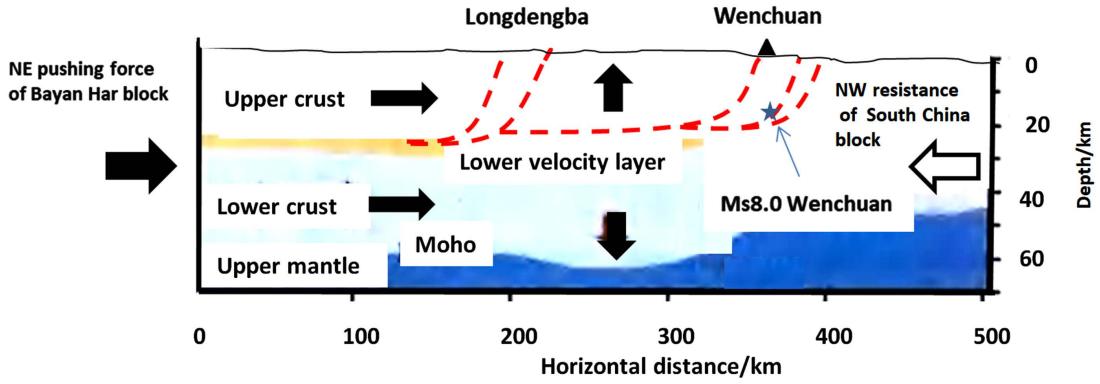

Figure 1. Location and tectonic setting of the Wenchuan deformation station (modified after Du *et al.* [23]).

There is no set definition for the area of pre-seismic stress field variation related to large earthquakes. Xu [25] found that strong earthquakes on the southeastern coast of China are characterized by circular seismotectonics, with the circular segment complementary to strong earthquakes on mainland China. Xu [26] suggested that the dynamic factors of the Wenchuan earthquake reflect seismicity related to the circum-Pacific seismic belt. In this study, we extended the geographical range of interest (15.0˚N - 41.5˚N, 82.0˚E - 123.5˚E) to include seismicity around Taiwan; this represents a greater geotechnical range than that used in most studies. Figure 2 shows the study area, including the distribution of $M_S \geq 5.5$ earthquakes that occurred between the 2001 Kunlun Mountain and 2008 Wenchuan earthquakes. The map shows increased seismicity in southwest China, South China, and around Taiwan. At the same time, an ellipse-shaped seismic gap (hereafter, a "gap ellipse") is also apparent (area within the red dashed line in Figure 2).

The M_S8.1 Kunlun earthquake epicenter was close to one end of the long axis of the gap ellipse. Enhanced post-seismic activity was centered around the Kunlun earthquake epicenter, and around Taiwan. The largest of these events occurred on 31 March 2002 (M_S7.5), 10 December 2003 (M_S7.0), and 26 December 2006 (M_S7.2). The epicenter of the Wenchuan earthquake was located in the center of the long axis of the ellipse; seismic activity was low before the earthquake.

A small number of CMONOC GNSS stations were established around the gap ellipse in 1999. The Luzhou (LUZH)-Guangzhou (GUAN) and Luzhou (LUZH)-Xiamen (XIAM) baselines are close to the long axis of the ellipse, the Luzhou (LUZH)-Delingha (DLHA) baseline connects the epicenters of the Kunlun Mountain and Wenchuan earthquakes, and the Luzhou (LUZH)-Kunming (KMIN) baseline is perpendicular to the long axis. Together, these baselines can reflect the characteristics of the stress field before the Wenchuan earthquake.

3. DATA AND ANALYSIS METHODS

3.1. Ground Tilt Data

We used ground tilt data from the Wenchuan deformation observation station. A quartz pendulum tiltmeter was used for continuous tilt observations before the Wenchuan earthquake. The instrument was located in a cave with a depth of 25 m, a covering layer of 40 m, and an annual temperature difference of less than 0.3˚C. The tiltmeter, which had a distance of 5.0 m between the light spot and rod, was placed on a marble pier and produced an analog record from manual hourly values. Since October 2002, the tiltmeter has recorded a normal pattern with a stable change curve. From tidal analysis of EW and NS tilt, we found that the change in the tidal factor was relatively stable. The errors in the tidal factor in the NS and EW directions were 0.019 and 0.094, respectively, and the relative errors were within 1%. From long-term ground tilt data, the annual variation law of NS tilt is good and there was no significant anomaly before

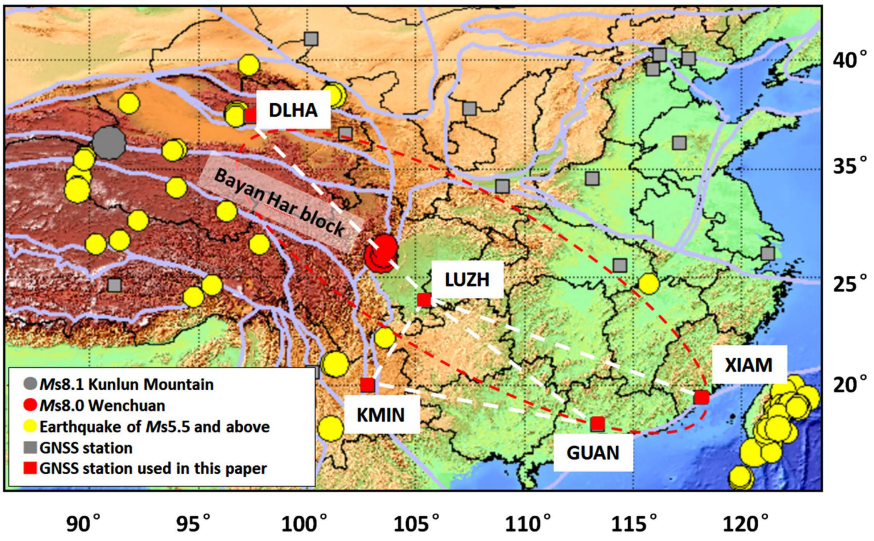

Figure 2. Distribution of $M_S \geq 5.5$ earthquakes between 14 November 2001 (M_S8.1 Kunlun Mountain earthquake) and 12 May 2008 (M_S8.0 Wenchuan earthquake). Squares denote the locations of permanent Global Navigation Satellite System (GNSS) stations of the Crustal Movement Observation Network of China (CMONOC). The red dashed ellipse represents the outline of a seismic gap; dashed white lines show the GNSS baselines used in this study; gray lines show the boundaries of secondary blocks.

the Wenchuan earthquake. In contrast, there was a significant change in the EW tilt. Owing to a westward blocking effect of the South China Plate, the EW tilt has dipped westward since the beginning of the observation period in October 2002.

3.2. Benioff Creep

To analyze the characteristics of seismicity before the Wenchuan earthquake, the strain energy released by the $M_S \geq 5.5$ earthquakes was calculated using the empirical formula of energy magnitude (1), taking a 1-month window length and 1-month sliding step length for data in the China earthquake catalogue [27]:

$$\log E = 1.5M_S + 4.8 \tag{1}$$

where E is the energy released by an earthquake with magnitude Ms. The cumulative Benioff creep at time t was calculated as follows [28]:

$$\varepsilon = \sum_i^{N_t} \sqrt{E_i} \tag{2}$$

where, N_t is the number of earthquakes occurring in the selected area before time t, and $\sqrt{E_i}$ is the Benioff creep of the i-th earthquake. Cumulative Benioff creep ε can reflect the level of seismic energy release from blocks or faults [29].

3.3. GNSS Baselines

Based on GNSS daily resolution results, several baselines around the gap ellipse were calculated, with the calculated length being the geodesic line between the two stations. The baseline length of the first day was set to zero so as to record relative change. At the same time, to filter out the influence of high-frequency information, the sixth order DB wavelet fitting result was adopted; that is, we filtered out high-frequency disturbances with periods of less than 64 days.

3.4. Fourier Spectrum Analysis

The discrete Fourier transform of a ground tilt data sequence $\{X(k)\}$ can be expressed as:

$$f_n = \frac{1}{N}\sum_{k=0}^{N-1} X(k) e^{-i\frac{2\pi k}{N}n}, \quad n = 0, \cdots, N-1 \tag{3}$$

where n is the discretization of the time domain and k is the discretization of the frequency domain; both are periodic at N points. For each frequency n, the square sum of the real and imaginary parts of f_n (*i.e.*, the spectral value) is the square of the wave amplitude corresponding to the frequency. The frequency or period corresponding to a higher spectrum value is the predominant period of the time series.

3.5. Correlation Analysis Method

Firstly, a time interval with a good change trend was selected as the benchmark, and linear models of the Benioff creep data and GNSS baseline data were established. Filtering was performed to obtain two nearly stable but abnormal residual sequences, and the simplest correlation model was selected. The GNSS baseline residual was taken as the dependent variable, and the Benioff creep residual was taken as the independent variable. A regression model was established to obtain the regression coefficient and fitting error between the two residual series. If more than 95% of points were less than 2 times the mean square deviation, a normal distribution was assumed and the model was considered to be accurate.

4. RESULTS

4.1. Ground Tilt in the Epicentral Area

Ground tilt observed at the Wenchuan station has obvious nonlinear characteristics that can be fitted by three linear segments with a reliability of α = 97.5% (**Figure 3**). The variation characteristics of these three stages are close to the gravity variation at the Yingxiu site, which is located on the same fault [30].

From October 2002 to the end of 2004 (moment A), the annual variation of the ground tilt showed stable westward movement; after moment A, the ground tilt rate decreased significantly, and the amplitude increased with time until the beginning of 2007 (moment B); from point B until to the Wenchuan earthquake (May 2008), the tilt rate was close to zero.

Fourier spectra of the linear change before point A and after point B were calculated (**Figure 4**). The peak spectral intensity occurred in a single year before moment A; however, the spectral intensity after point B was obviously lower. These results show that the amplitude of the main periodic wave decreased as the occurrence time of the Wenchuan earthquake approached.

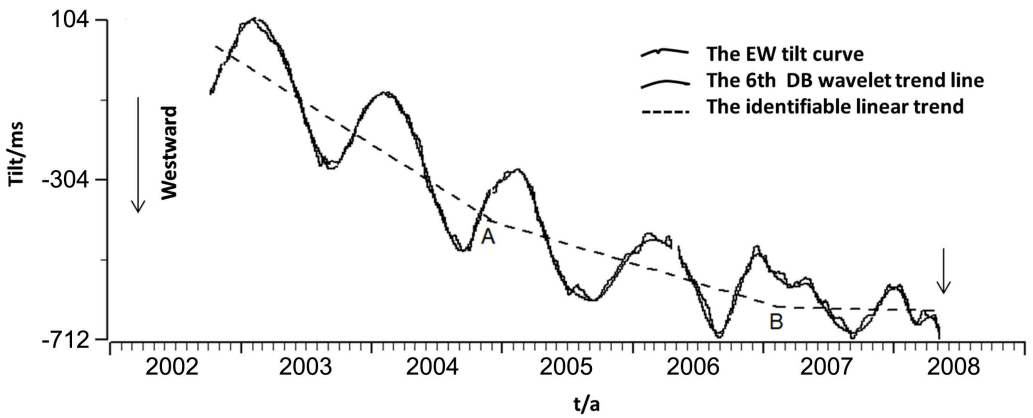

Figure 3. Variation in EW tilt observed at the Wenchuan deformation station. A and B mark turning points in the rate of change; the arrow indicates the occurrence of the Wenchuan earthquake.

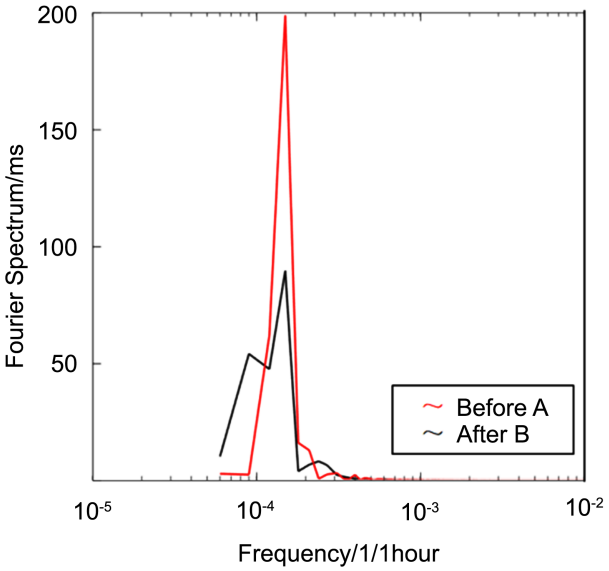

Figure 4. Periodic spectra before moment A (at the end of 2004) and after moment B (at the beginning of 2007).

4.2. Peripheral Benioff Creep

According to the Benioff creep calculation (**Figure 5**), after the M_S8.1 Kunlun Mountain earthquake, the release rate of seismic energy accelerated until mid-2004 (point A), after which it fell significantly, showing a long-term "deficit"; in the middle of 2007 (point B), which is regarded as the sub-instability stage [31], the release of seismic strain energy again increased until the Wenchuan earthquake.

4.3. GNSS Baseline Analysis

The permanent LUZH GNSS station is ~200 km away from the Wenchuan earthquake epicenter. The LUZH-DLHA baseline approximately follows the direction of the major axis of the gap ellipse, and connects the active areas of the Kunlun Mountain and Wenchuan earthquakes. Over the long-term, the baseline has been in a state of extension (**Figure 6(a)**), reflecting the joint action of the Indian and Eurasian plates, with the Bayan Har block compressed in the NE direction, and the Sichuan-Yunnan region experiencing a dextral escape. However, in the 2 months preceding the Wenchuan earthquake, the baseline experienced shortening. A similar phenomenon also occurred before the Kunlun Mountain earthquake in 2001; at the end of July 2001, a significant reverse acceleration lasted for 3 months, with the earthquake marking the end of the acceleration process and a return to the original pre-seismic trend. Therefore, from the perspective of large-scale GNSS baseline variation, it is possible to identify far-field pre-seismic instability.

The LUZH-KMIN baseline, which is approximately perpendicular to the major axis of the gap ellipse, showed a decrease in the rate of extension from the beginning of 2007 until the Wenchuan earthquake (**Figure 6(b)**).

The XIAM GNSS station is located on the southeast coast of China, close to Taiwan. Taiwan sits at the junction of the Philippines and Ryukyu subduction tectonic belts. The southern and northern ends of Taiwan island are connected by NW trending transfer faults. Owing to the collision of the Philippine Sea Plate and Eurasian Plate, a compressional tectonic deformation zone, mainly represented by the central mountains, has formed on Taiwan island; this zone has a large number of NE nearly north-south imbricate thrust or overthrust structures, and intense tectonic deformation and seismic activity. These processes also affect the Taiwan Strait and southeast coast [32, 33]. As shown in **Figure 7(a)**, seismicity around Taiwan occurs in temporal clusters. Earthquakes of $M_S \geq 5.5$ were concentrated in mid 2002, the end of 2003

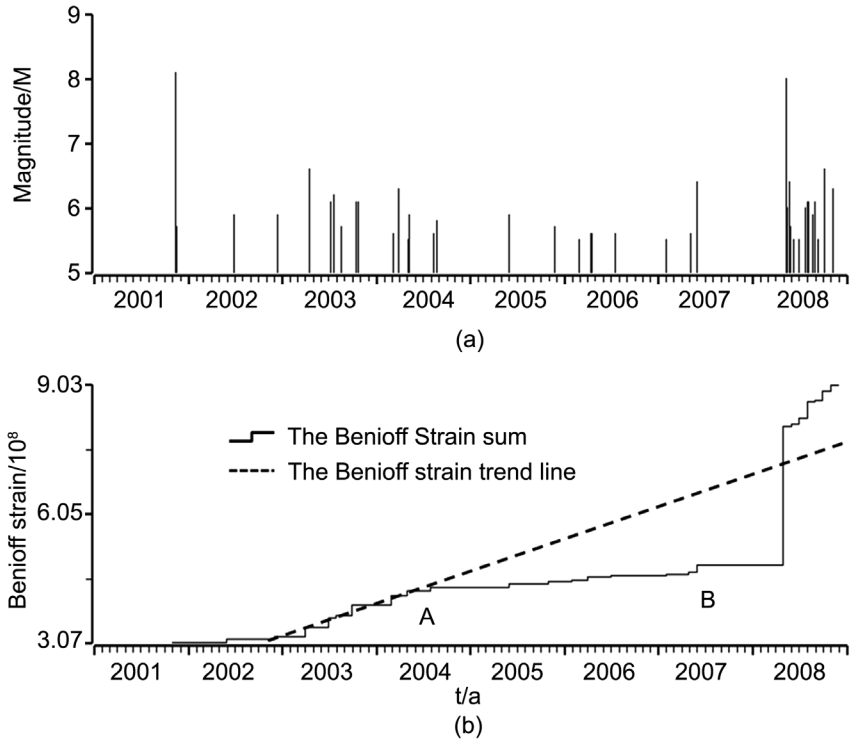

Figure 5. (a) M-t of $M_S \geq 5.5$ earthquakes before and after the Wenchuan earthquake and (b) the corresponding Benioff creep.

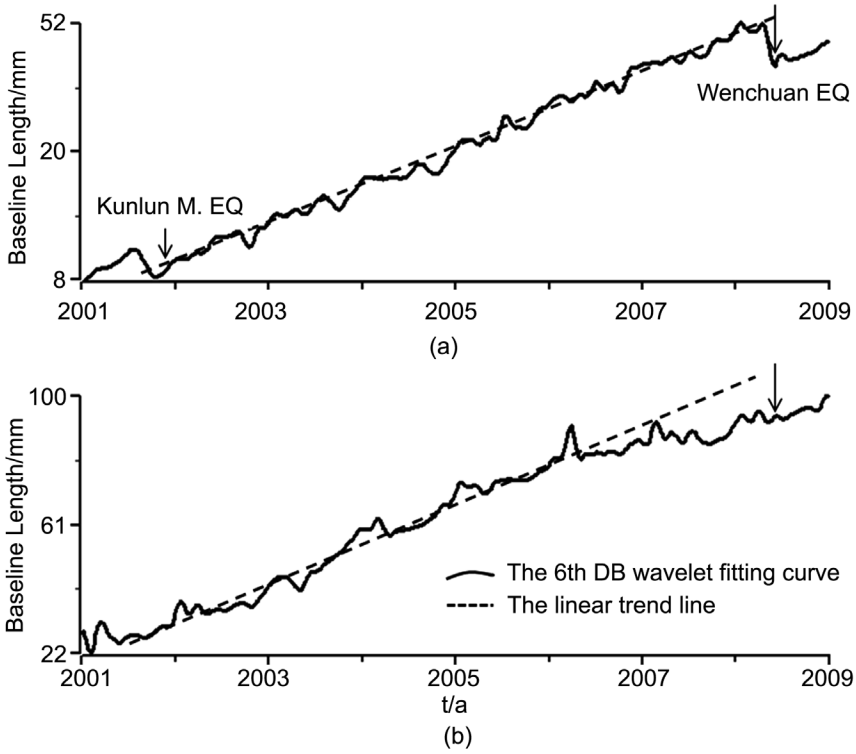

Figure 6. Changes in the (a) LUZH-DLHA and (b) LUZH-KMIN Global Navigation Satellite System (GNSS) baselines from 2001 to 2009.

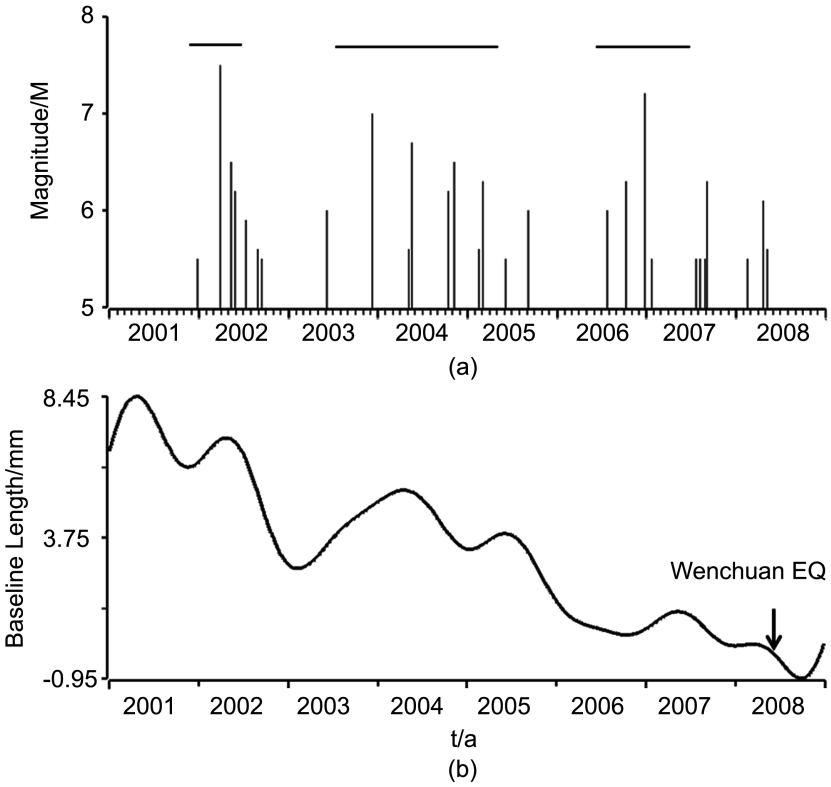

Figure 7. (a) *M*-t of earthquakes in Taiwan and (b) changes in the LUZH-XIAM Global Navigation Satellite System (GNSS) baseline length from 2001 to 2008.

to mid 2005, and the end of 2006 to mid 2007. The LUZH-XIAM baseline extends approximately along the major axis of the gap ellipse; it mainly exhibits compression owing to the NW compression and collision of the Philippine Plate and the NW compression of the Indian Plate. During the intervals between these clusters, the baseline experienced rapid changes in compression (Figure 7(b)), suggesting that compression processes control Taiwan earthquakes; however, there was no significant change in the baseline before the Wenchuan earthquake.

The LUZH-GUAN baseline changed significantly before the Wenchuan earthquake. From early 2005 to mid 2007 it experienced rapid compression, which is rare in South China. However, from the end of 2007 until the Wenchuan earthquake the baseline experienced extension (Figure 8). This indicates that the Philippines Plate has enhanced the Chinese mainland plate, and is less affected by Taiwan earthquakes. The GUAN-KMIN baseline extends approximately parallel to the LUZH-XIAM baseline; similarly, no significant changes occurred before the Wenchuan earthquake.

4.4. Correlation between LUZH-GUAN Baseline Shortening and Benioff Creep Deficit

By comparing the variations in the Benioff creep (Figure 5(b)) and LUZH-GUAN baseline (Figure 8) prior to the Wenchuan earthquake, we found that the start and end times of the pre-seismic anomalies were similar; moreover, the amplitudes of both were relatively significant, and the variation characteristics were similar.

To investigate this further, we converted the daily LUZH-GUAN baseline data into monthly sampling, with 1 sample per month. November 2001 was taken as the first value, $i = 1$; the Wenchuan earthquake month was $i = 79$, and December 2008 was the last month in the analysis ($i = 86$).

Based on the baseline and Benioff creep data before December 2004, a linear model was constructed and filtered to obtain the residual dL_i, $d\varepsilon_i$:

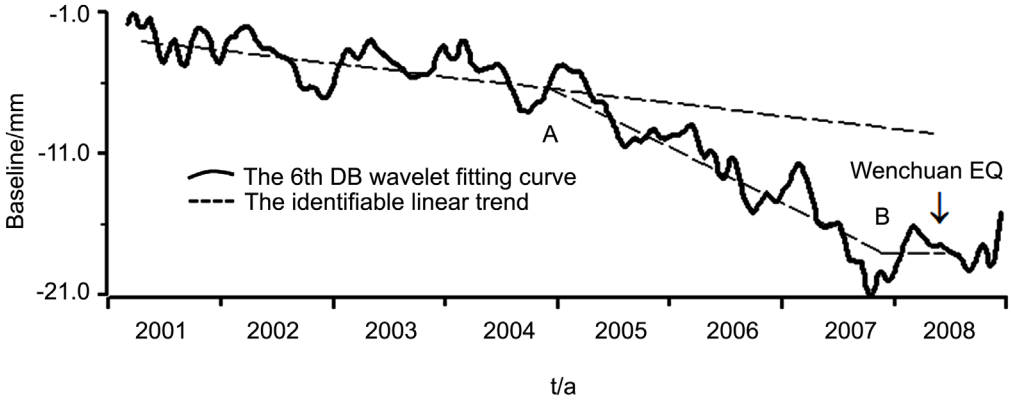

Figure 8. Variation in the LUZH-GUAN Global Navigation Satellite System (GNSS) baseline length from 2001 to 2008. A and B mark turning points in the rate change.

$$dL_i = \Delta L_i - (0.077 \cdot i - 3.584) \tag{4}$$

$$d\varepsilon_i = \varepsilon_i - (0.0552 \cdot i + 2.7478) \tag{5}$$

where, L_i and dL_i are the baseline relative value and residual value, respectively (both in mm); and $\varepsilon_i, d\varepsilon_i$ are the standardized Benioff creep and linear filtering residual values, respectively (both in 10^8).

Correlation analysis yielded the following formulas:

$$dL_i = 6.0 \cdot d\varepsilon_i + \Delta_i, \ i = 1\text{-}78 \tag{6}$$

$$\Delta_i = dL_i - 6.0 \cdot d\varepsilon_i, \ i = 1\text{-}78 \tag{7}$$

where Δ_i is the fitting error of the LUZH-GUAN GNSS baseline based on seismic strain; its root mean square error is 1.7 mm and it obeys a normal distribution with 96.2% probability. According to the fitting results given in **Figure 9**, there was a strong correlation between earthquake creep and the GNSS baseline shortening before the Wenchuan earthquake ($i < 79$). That is, there is evidence of a link between the accumulated energy of crustal strain and the release of energy during the earthquake.

After the Wenchuan earthquake, assuming that 50% of the earthquake energy was converted into strain energy, an energy balance can still be achieved with the model (8):

$$\Delta_i = dL_i + 3.0 \cdot d\varepsilon_i, \ i = 79\text{-}86 \tag{8}$$

The linear balance results are shown in **Figure 9**. The mean value of Δ_i over the whole process was zero, and the fitting error was 1.68 mm; the data obey a normal distribution with 96.55% reliability. In summary, our results show that the accumulation of strain energy (expressed as the shortening of the baseline) before the earthquake was balanced by the release of seismic strain energy during and after the earthquake.

5. DISCUSSION AND CONCLUSIONS

By analyzing tilt data from the epicenter area, along with GNSS baseline and seismicity data from peripheral and distal regions, we obtained far- and near-field crustal deformation information for before and after the Wenchuan earthquake. From our analysis, we identified the distribution characteristics of crustal stress field changes before the earthquake, which provides an important basis for understanding the significance of geophysical field observations and for improving the layout of observation networks.

The ground tilt changes observed near the epicenter of the Wenchuan earthquake are consistent with normal pre-earthquake deformation, including a linear loading process (α), nonlinear strain accumulation (β), and pre-seismic sub-instability (γ). The linear loading process was consistent with the background

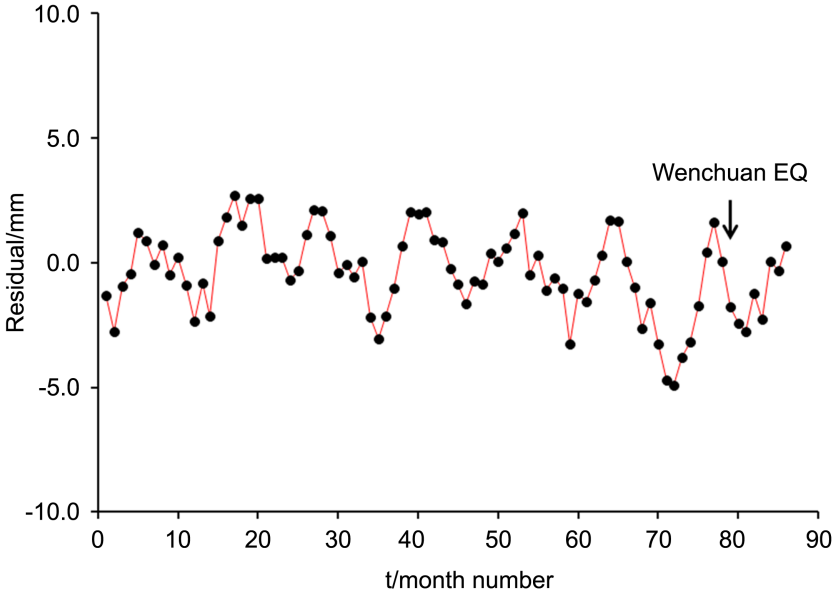

Figure 9. Balance between the shortening of the LUZH-GUAN GNSS Global Navigation Satellite System (GNSS) baseline and the earthquake strain anomaly.

stress of the Wenchuan station, and the westward tilt reflects the joint action of Indian Plate compression and South China Plate resistance. The nonlinear change mainly reflects a slowing of the change rate, indicating a significant change in crustal properties or in the strain accumulation [34]. During the sub-instability stage, the seismogenic fault was locked, and the amplitude of deformation for some of the main period decreased significantly.

The characteristics of the pre-seismic sub-instability deformation identified in this study differ from the current understanding, and the sub-instability differed from the instability. Before and after the sub-instability stage, different structural areas played different roles in deformation. Based on 40 years of tilt and strain from Japan, Takemoto [10] proposed that the distributions of precursor ground deformation anomalies are localized. Close to the epicenter, precursors are rare, with a minimum precursor distance of ~60 km. Based on analysis of deformation before the Tangshan and Songpan earthquakes, Ma *et al.* [35] found a deviation between precursors and rupture sites. That is, significant pre-seismic deformation is often far from the eventual epicenter; the epicenter area has the least amount of deformation; this conclusion was verified experimentally. Other experimental studies on fault action patterns have shown that creep slip anomalies occur along faults under compression, and that the fracture usually occurs on a fault that obliquely intersects that exhibiting the anomaly [36, 37]. Pre-seismic deformation in the epicentral region of the Wenchuan earthquake confirms that the seismogenic fault was in a highly locked state during the sub-instability stage. The epicenter is often the fixed point for regional deformation [12], and this is an important reason for the lack of precursory deformation driven by deep stress [3].

During strain energy accumulation, the change in the ground tilt of the Wenchuan earthquake epicenter area, the seismicity in surrounding area, and the change along large-scale GNSS baselines showed strong synergistic characteristics. Points A and B (marked in **Figure 2**, **Figure 5**, and **Figure 8**) were turning points for major anomalies that occurred relatively close in time. At time point A, there were synchronous accelerations in the "deficit" of Benioff creep release, the shortening of the LUZH-GUAN GNSS baseline, and the deceleration of the ground tilt rate in the epicenter area; this indicates that there was energy exchange between the far- and near-fields. At the same time, there was a strong correlation between the reduction in Benioff creep release and shortening of the LUZH-GUAN GNSS baseline, which suggests a balance between crustal strain energy accumulation and seismic energy release. Zhang *et al.* [38] showed that there is a linear relationship between the level of seismicity and the tectonic activity rate in the

boundary zone; to a certain extent, this also manifests as a strong correlation between strain accumulation and seismicity. After time point B, the tilt rate was almost zero, the release of Benioff creep energy was low, and the LUZH-GUAN GNSS baseline became stable (after a period of accelerated shortening); these phenomena reflect pre-seismic stress field changes owing to the sub-instability stage that preceded the Wenchuan earthquake.

Our results confirm that before some large earthquakes, it is difficult to observe accelerated deformation near the epicenter; however, observations in peripheral and distal areas may be more prominent. The Kunlun Mountain and Wenchuan earthquakes both occurred when long-term extension of the LUZH-DLHA GNSS baseline was reversed (*i.e.*, there was a period of shortening); the Kunlun Mountain and Wenchuan epicenters were close to the DLHA and LUZH GNSS stations, respectively. This indicates that far-field stress disturbances may directly trigger some large earthquakes.

Finally, owing to the influence of deep fluid or plastic material flow, deformation observed under natural conditions usually reflects changes in the stress-strain field, and is characterized by spatial migration; therefore, it differs from coseismic deformation. Moreover, our results are also in contrast to the generally accepted understanding of crustal deformation characteristics before large earthquakes. The results of this study have significance for the improved understanding of geophysical field observations and the complexity of earthquake precursors; moreover, the results will help in innovating the idea of earthquake prediction.

ACKNOWLEDGEMENTS

We thank the First Monitoring and Application Center of the China Earthquake Administration for providing the GPS time series datasets. This research was funded by the National Key R&D Program of China, grant number 2018YFC1503606, and the National Natural Science Foundation of China, grant number 41330314.

CONFLICTS OF INTEREST

The authors declare no conflicts of interest regarding the publication of this paper.

REFERENCES

1. Xu, X.W., Wen, X.Z., Ye, J.Q., Ma, B.Q., Chen, J., Zhou, R.J., He, H.L., Tian, Q.J., He, Y.L., Wang, Z.C., Sun, Z.M., Feng, X.J., Yu, G.H., Chen, L.C., Chen, G.H., Yu, S.E., Ran, Y.K., Li, X.G., Li, C.X. and An, Y.F. (2008) The M_S8.0 Wenchuan Earthquake Surface Ruptures and Its Seismogenic Structure. *Seismology and Geophysics*, **30**, 597-629. (In Chinese)
2. Wen, X.Z., Zhang, P.Z., Du, F. and Long, F. (2009) The Background of Historical and Modern Seismic Activities of the Occurrence of the 2008 M_S8.0 Wenchuan, Sichuan, Earthquake. *Chinese Journal of Geophysics*, **52**, 444-454. (In Chinese)
3. Teng, J.W., Bai, D.H., Yang, H., Yan, Y.F., Zhang, H.S., Zhang, Y.Q. and Ruan, X.M. (2008) Deep Processes and Dynamic Responses Associated with the Wenchuan M_S8.0 Earthquake of 2008. *Chinese Journal of Geophysics*, **51**, 1385-1402. (In Chinese) https://doi.org/10.1002/cjg2.1347
4. Bilham, R. (2005) Co-Seismic Strain and the Transition to Surface after Slip Recorded by Creep-Meters near the 2004 Parkfield Epicenter. *Seismological Research Letters*, **76**, 49-57. https://doi.org/10.1785/gssrl.76.1.49
5. Johnston, M.J.S., Borcherdt, R.D., Linde, A.T. and Gladwin, M.T. (2006) Continuous Borehole Strain and Pore Pressure in the Near Field of the 28 September 2004 M6.0 Parkfield, California, Earthquake: Implications for Nucleation, Fault Response, Earthquake Prediction, and Tremor. *Bulletin of the Seismological Society of America*, **96**, S56-S72. https://doi.org/10.1785/0120050822
6. Amoruso, A. and Crescentini, L. (2010) Limits on Earthquake Nucleation and Other Pre-Seismic Phenomena

from Continuous Strain in the Near Field of the 2009 L'Aquila Earthquake. *Geophysical Research Letters*, **37**, L10307. https://doi.org/10.1029/2010GL043308

7. Rice, J.R. and Rudnicki, J.W. (1979) Earthquake Precursory Effects Due to Pore Fluid Stabilization of a Weakened Fault Zone. *Journal of Geophysical Research*, **84**, 2177-2184. https://doi.org/10.1029/JB084iB05p02177
8. Fang, Z.J., Dieterich, J.H. and Xu, G. (2010) Effect of Initial Conditions and Loading Path on Earthquake Nucleation. *Journal of Geophysical Research*, **115**, B06313. https://doi.org/10.1029/2009JB006558
9. Fu, H. and Liu, J. (2018) Significant Anomalies of Precursory Observation before Wenchuan Earthquake and Their Physical Basis. *Recent Developments in World Seismology*, **8**, 29. (In Chinese)
10. Takemoto, S. (1991) Some Problems on Detection of Earthquake Precursors by Means of Continuous Monitoring of Crustal Strains and Tilts. *Journal of Geophysical Research*, **96**, 10377-10390. https://doi.org/10.1029/91JB00239
11. Bakun, W.H., Aaggard, B., Dost, B., Ellsworth, W.L., Hardebeck, J.L., Harris, R.A., Ji, C., Johnston, M.J.S., Langbein, J., Lienkaemper, J.J., Michael, A.J., Murray, J.R., Nadeau, R.M., Reasenberg, R.M., Reichle, M.S., Roeloffs, E.A., Shakal, A., Simpson, R.W. and Waldhauser, F. (2005) Implications for Prediction and Hazard Assessment from the 2004 Parkfield Earthquake. *Nature*, **437**, 969-974. https://doi.org/10.1038/nature04067
12. Niu, A.F., Zhang, L.K., Zhang, J., Li, Y., Zhao, J., Yan, W., Yue, C. and Yuan, Z. (2020) On the Fixed Points in Crust Deformation Prior to Wenchuan Earthquake and Dynamic Background. *J. Geod. Geodyn.*, **40**, 1-6. (In Chinese)
13. Scholz, C.H. (1978) A Physical Interpretation of the Haicheng Earthquake Prediction. *Nature*, **267**, 121-124. https://doi.org/10.1038/267121a0
14. Feng, D.Y., Pan, Q.L., Zheng, S.H., Xue, F. and Min, X.Y. (1984) Long-Period Deformation Waves and Short-Term and Imminent Earthquake Precursors. *Acta Seismologica Sinica*, **6**, 41-57. (In Chinese)
15. Wang, S.J. and Yin, Z.S. (1989) Long Period Deformation Waves and Slow Earthquakes. *Crustal Deformation and Earthquakes*, **9**, 1-10. (In Chinese)
16. Niu, A.F. (2017) Crust Stress Waves and Its Applications in Earthquake Prediction. Seismol. Press, Beijing. (In Chinese)
17. Wu, Y.L., Li, P., Chen, G.Q. and Li, X.D. (1992) Inversion of the Strain Accumulation State in Crustal Interior from Observations of Earth Tide Tilts. *China Earthq.*, **8**, 62-67. (In Chinese)
18. Ma, J. and Guo, Y.S. (2014) Accelerated Synergism Prior to Fault Instability: Evidence from Laboratory Experiments and an Earthquake Case. *Seismology and Geophysics*, **36**, 547-561. (In Chinese)
19. Ma, J. (2016) On "Whether Earthquake Precursors Help for Prediction Do Exist". *Chinese Science Bulletin*, **61**, 409-414. (In Chinese) https://doi.org/10.1360/N972015-01239
20. Ren, Y.Q., Liu, P.X., Ma, J. and Chen, S.Y. (2013) An Experimental Study on Evolution of the Thermal Field of en Echelon Faults during the Meta-Instability Stage. *Chinese Journal of Geophysics*, **56**, 2348-2357. (In Chinese)
21. Niu, A.F., Gu, G.H., Cao, J.P., Zhang, L., Yan, W., Zhao, J. and Ji, P. (2013) On the Preseismic Deformation Changes Prior to the Lushan M_S7.0 Earthquake. *Acta Seismologica Sinica*, **35**, 670-680. (In Chinese)
22. Zhang, X., Liu, X., Qin, S.L. and Jia, P. (2020) Precursory Characteristics of Meta-Instability of Cross-Fault Deformation before Lushan M_S7.0 Earthquake. *Geomat. Inf. Sci. Wuhan Univ.*, **45**, 1669-1677. (In Chinese)
23. Du, F., Wen, X.Z., Zhang, P.Z. and Wang, Q.L. (2009) Interseismic Deformation across the Longmenshan Fault Zone before the 2008 M8.0 Wenchuan Earthquake. *Chinese Journal of Geophysics*, **52**, 2729-2738. (In Chinese)
24. Zhang. Y.S., Zheng, X.J. and Wang, L.M. (2016) The Distribution Characteristics of Deformation Field Caused by Three Great Earthquakes in the Qinghai-Tibet Plateau and Its Vicinity since 2001. *Chinese Journal of Geophysics*, **59**, 3637-3645. (In Chinese)

25. Xu, S.X. (2005) Correlation and Tectonic Characteristics of Great Earthquake Group Quanzhou-Qiongshan at Beginning of 17 Century. *J. Geod. Dyn.*, **25**, 1-5. (In Chinese)

26. Xu, S.X. (2009) On the Characteristic of Large Scale and Deep Layer on Dynamic Force of Earthquake Occurrence, Based on the Phenomena before Wenchuan Earthquake. *Engineering Science*, **11**, 16-18. (In Chinese)

27. Kanamori, H. (1977) The Energy Release in Great Earthquakes. *Journal of Geophysical Research*, **82**, 2981-2987. https://doi.org/10.1029/JB082i020p02981

28. Benioff, H. (1951) Earthquakes and Rock Creep: Part 1: Creep Characteristics of Rocks and the Origin of Aftershocks. *Bulletin of the Seismological Society of America*, **41**, 31-42. https://doi.org/10.1785/BSSA0410010031

29. Song, C.Y., Ma, J., Wang, H.T. and Zhang, L.L. (2018) Study on Meta-Instability Stage and Instable Section of the Fault before Strong Earthquake: Taking Western Section of Southern Tianshan as an Example. *Chinese Journal of Geophysics*, **61**, 604-615. (In Chinese)

30. Zhu, Y.Q., Xu, Y.M., Lu, Y.P. and Li, T.M. (2009) Relations between Gravity Variation of Longmenshan Fault Zone and Wenchuan M8.0 Earthquake. *Chinese Journal of Geophysics*, **52**, 2538-2546. (In Chinese)

31. Wang, K.Y., Guo, Y.S. and Feng, X.D. (2018) Sub-Instability Stress State Prior to the 2008 Wenchuan Earthquake from Temporal and Spatial Stress Evolution. *Chinese Journal of Geophysics*, **61**, 1883-1890. (In Chinese)

32. Peng, F.N. and Ye, Y.C. (2004) Seismogenic Fault of the 1999 Chi-Chi Earthquake in Taiwan Province and the Features of Earthquake Damages. *Seismology and Geophysics*, **26**, 576-585

33. Zhang, Z.Z., Pan, H., Huang, Z., Wang, S.Y., You, L.B., Er, J.Q. and Wu, X. (2009) Impacts of the Taiwan and Taiwan Strait Earthquakes on China Mainland. *Acta Seismologica Sinica*, **31**, 319-332.

34. Dubrovolsky, I.P., Zubkov, S.I. and Miachin, V.I. (1979) Estimation of the Size of the Earthquake Preparation Zones. *Pure and Applied Geophysics*, **117**, 1025-1044. https://doi.org/10.1007/BF00876083

35. Ma, J., Liu, L.Q. and Ma, S.L. (1999) Fault Geometry and Departure of Precursors from Epicenter. *Earthq. Res. China*, **15**, 106-115. (In Chinese)

36. Ma, J. and Ma, S.L. (2000) Experimental Study on Alternate Slip of Interseismic Faults and Block Movement. *Seismology and Geophysics*, **22**, 65-73. (In Chinese)

37. Ma, J., Ma, S.L., Liu, L.Q., Wang, K.Y. and Hu, X.Y. (2002) Experimental Study on Interaction Patterns of Faults. *Progress in Natural Science*, **12**, 503-508. (In Chinese)

38. Zhang, G.M., Ma, H.S., Wang, H. and Wang, X.L. (2005) Boundaries between Active-Tectonic Blocks and Strong Earthquakes in the China Mainland. *Chinese Journal of Geophysics*, **48**, 602-610. (In Chinese) https://doi.org/10.1002/cjg2.699